Distributed Strain Sensing with Long Gauge FBG Sensors Based on Optical Frequency Domain Reflectometry

H. MURAYAMA, H. IGAWA, K. KAGEYAMA, I. OHSAWA, K. UZAWA,

M. KANAI, S. KOBAYASHI AND T. SHIRAI

ABSTRACT:

A quasi-distributed sensing system with fiber Bragg grating (FBG) sensors can be useful for monitoring comprehensive deformation by measuring strain in a structure. However, initial damage, such as crack, may generate not an abnormal deformation but just a local perturbation in a stress distribution. If the area of the perturbation is much smaller than the gauge length of the FBG sensor, we will obtain an averaged strain value from an interrogation system of FBG sensors. Some interrogation system may give us an abnormal one which cannot be quantitatively evaluated or is meaningless. Therefore, a strain sensing system with the higher spatial resolution and accuracy is required to detect damage reliably and estimate the remaining strength of a structure. In this paper we show that the distributed strain measurements with the high spatial resolution can be implemented by the new sensing technique based on optical frequency domain reflectometry (OFDR). We could easily map the strain profile along a FBG from a spectrogram calculated by applying Fourier transform analysis with a sliding window to the signal obtained from the measurement system. The signal obtained from the measurement system can be simulated by the transfer matrix method based on coupled mode theory. In the experiments, we used also a long gauge FBG sensor whose gauge length is 50 or 100 mm as well as an ordinary one whose gauge length is 10 mm. The strain distribution adjacent to holes of an aluminum tensile specimen was measured by a 10 mm FBG with the polyimide coating and a 50 mm FBG with the acrylate coating. The agreement between the experimental result of the polyimide coating FBG and the simulated one was good. This means that the simulation model was reasonable and can be used to design a measurement system with higher performance. However, we could not accurately measure strain varying sharply near the hole by the acrylate coating FBG.

H. Murayama, K. Kageyama, I. Ohwasa, K. Uzawa, M. Kanai and S. Kobayashi, School of Engineering, the University of Tokyo, 7-3-1 Hongo, Bunkyo-ku, Tokyo 113-8656, Japan, e-mail: murayama@giso.t.u-tokyo.ac.jp
H. Igawa, Institute of Aerospace Technology, Japan Aerospace Exploration Agency, 6-13-1 Ohsawa, Mitaka, Tokyo 181-0015, Japan
T. Shirai, Lazoc Inc., 3-40-9 Hongo, Bunkyo-ku, Tokyo 113-0033, Japan

INTRODUCTION

Fiber Bragg grating (FBG) sensors are used to measure strain or temperature in structural sensing applications. Quasi-distributed sensing can be implemented by FBG sensors which are discretely located along an optical fiber. Various techniques for interrogating FBG sensors have been developed and they are capable of simultaneously monitoring a number of FBG elements [1]. In general, such a quasi-distributed sensing system with FBG sensors can be useful for monitoring deformation and assessing the stiffness of a structural member or the whole structure. However, initial damage, such as crack or debonding, may generate not an abnormal deformation but just a local perturbation in a stress distribution. If the area of the perturbation is much smaller than the gauge length of the FBG sensor that is ordinarily about 10 mm, we will obtain an strain value averaged within the gauge length from an interrogation system of FBG sensors. Some interrogation systems may give us an abnormal one which cannot be quantitatively evaluated or is meaningless. Therefore, a strain sensing system with the higher spatial resolution and accuracy is required in order to detect damage reliably and estimate the remaining strength of a structure.

While FBG sensors with some interrogation systems are ordinarily employed for quasi-distributed strain or temperature measurements, they can be also applied to full-distributed sensing. In recent years various techniques for distributed strain measurements by using FBG have been proposed. If a strain distribution measured is monotonic, the strain profile along the grating can be determined by analyzing the reflection spectrum [2]. A strain distribution along a chirped grating can be measured by the phase-based sensing method or the low-coherence reflectometry [3,4]. However, these distributed sensing methods have a drawback, such as elimination of uniform gratings or short sensing range. By using a tunable laser demodulation, the strain profile along a uniform grating with a long gauge length can be mapped based on Fourier transform analysis [5]. Although this sensing system can measure strain distributions with the high spatial resolution, it seems that signals outputted from several photodetectors in the sensing system have to be acquired individually and analyzed step by step. In this paper we show that the distributed strain measurements with the high spatial resolution can be implemented by the new sensing technique based on optical frequency domain reflectometry (OFDR) [6].

In quasi-distributed strain measurements OFDR can be used to determine the wavelength of light reflected from hundreds of low reflectivity FBGs distributed along an optical fiber [7]. The signal at the photodetector in the interferometer consisted of a mirror end and FBG array is acquired at the constant wavenumber interval while the wavelength (wavenumber) of the laser light from the tunable laser is swept. The Fourier transform of the signal sampled at the constant wavenumber interval provides the information on the position of each FBG in the array, and a narrow inverse Fourier transform at specific positions (frequencies) within this Fourier transform can then be used to recover the wavelength spectrum of a specific FBG.

On the other hand, in the distributed measurement using OFDR, we can easily map the strain profile along a long gauge FBG or FBG array from a spectrogram given by applying Fourier transform analysis with a sliding window to the signal at the photodetecter in the measurement system whose layout is similar to that of Ref. [7]. The

signal in the interferometer with a mirror end and FBG sensors can be simulated by the transfer matrix method based on coupled mode theory [8, 9]. In the experiments, we used also a long gauge FBG sensor whose gauge length is 50 or 100 mm as well as an ordinary one whose gauge length is 10 mm. The strain distribution adjacent to holes of an aluminum tensile specimen was measured by a 10 mm FBG with the polyimide coating and a 50 mm FBG with the acrylate coating. The agreement between the experimental result of the polyimide coating FBG and the simulated one was good. This means that the simulation model was reasonable and can be used to design a measurement system with higher performance. However, we could not accurately measure strain varying sharply near the hole by the acrylate coating FBG. It is supposed that the interface between the cladding and the coating was affecting the spatial resolution in distributed strain sensing.

PRINCIPLE AND SIMULATION MODEL OF DISTRIBUTED STRAIN SENSING WITH FBG SENSORS BASED ON OFDR

Optical system and data acquisition

The measurement system with OFDR consists of a wavelength tunable laser (ANDO AQ4321A), three 3dB couplers (C1, C2, C3), two photodetectors (D1, D2), three broadband reflectors (R1, R2, R3), FBG sensors and a Pentium PC installed a A/D converter (National Instruments PCI 6115) and data acquisition/processing program written in LabVIEW. The arrangement with a long gauge FBG is shown in Fig. 1.

The laser light from the tunable laser is split by C1 and travels to C2 and C3. C2 is used to form an in-fiber interferometer with the light reflected R1 and R2, detected at D1. This interferometer has an optical path length difference of $2nL_R$ where n is the effective refractive index and L_R is the path difference of the two paths through the interferometer. The reflected lights from R1 and R2, RL_{R1} and RL_{R2}, are given by

$$RL_{R1} = \exp\{i(2nL_{R1}k + \pi)\} \tag{1}$$

$$RL_{R2} = \exp\{i(2nL_{R2}k + \pi)\} \tag{2}$$

where L_{R1} is the distance between D1 and R1 as well as L_{R2} is that between D1 and R2. Therefore, the difference between L_{R2} and L_{R1} is equal to L_R. Additionally, k is the wavenumber of the light and is related to the wavelength λ and given by the following equation.

$$k = \frac{2\pi}{\lambda} \tag{3}$$

The signal at D1 is given by the following equation.

$$\begin{aligned} D_1 &= (RL_{R1} + RL_{R2})(RL_{R1} + RL_{R2})^* \\ &= 2\{1 + \cos(2nL_R k)\} \end{aligned} \tag{4}$$

As the laser is tuned, Eq. (4) implies light intensity observed by D1 varies in a cycle depending on a wavenumber change, Δk, of the following equation.

$$\Delta k = \frac{\pi}{nL_R} \tag{5}$$

The positive going zero crossing of the signal at D1 is used to trigger the sampling of the signal at D2. C3 is used to form an in-fiber interferometer with the light reflected R3 and the long gauge FBG as well as C2 is. Therefore, the signal at D2 is given by

$$D_2 = \left(RL_{R3} + RL_{FBG}\right)\left(RL_{R3} + RL_{FBG}\right)^* \tag{6}$$

where RL_{R3} and RL_{FBG} are reflected lights from R3 and the grating, respectively. RL_{R3} is given by

$$RL_{R3} = \exp\{i(2nL_{R3} + \pi)\} \tag{7}$$

where L_{R3} is the distance between D2 and R3. RL_{FBG} can be determined by the transfer matrix method based on coupled mode theory [10]. First, we divide the grating with the gauge length of L into M uniform sections whose length is Δz as shown in Fig. 2. The reflection characteristic of each section is regarded as uniform within the length of Δz. The input/output relationship for the interferometer system of Fig. 2 is given by

$$\begin{bmatrix} R_0 \\ S_0 \end{bmatrix} = \mathbf{T}\begin{bmatrix} R_M \\ S_M \end{bmatrix}; \quad \mathbf{T} = \mathbf{P_G} \cdot \mathbf{F_1} \cdot \mathbf{F_2} \cdots \mathbf{F_i} \cdots \mathbf{F_M} \tag{8}$$

where R_0 and R_M are the amplitudes of the forward propagating mode at the end of the detector side and the another end, respectively. S_0 and S_M are the amplitudes of the backward propagating mode at the end of the detector side and the other side, respectively. The components of $\mathbf{F_i}$ and the phase-shift matrix, $\mathbf{P_G}$, are given by

$$\mathbf{F_i} = \begin{bmatrix} \cosh(\gamma_B \Delta z) - i\dfrac{\hat{\sigma}}{\gamma_B}\sinh(\gamma_B \Delta z) & -i\dfrac{\kappa}{\gamma_B}\sinh(\gamma_B \Delta z) \\ i\dfrac{\kappa}{\gamma_B}\sinh(\gamma_B \Delta z) & \cosh(\gamma_B \Delta z) + i\dfrac{\hat{\sigma}}{\gamma_B}\sinh(\gamma_B \Delta z) \end{bmatrix} \tag{9}$$

$$\mathbf{P_G} = \begin{bmatrix} \exp\{-in(L_{R3} + L_G)k\} & 0 \\ 0 & \exp\{in(L_{R3} + L_G)k\} \end{bmatrix} \tag{10}$$

where $\hat{\sigma}$ and κ are the general "dc" self-coupling coefficient and the "ac" coupling coefficient, respectively, and $\gamma_B = \sqrt{\kappa^2 - \hat{\sigma}^2}$ [13]. L_G is the distance between R3 and the end of the detector side in the grating. Finally, when the boundary conditions ($R_0 = 1$ and $S_M = 0$) are applied to Eq. (8), we find

$$RL_{FBG} = S_0 = \frac{T_{21}}{T_{11}} \tag{11}$$

The D2 signal sampled at the constant wavenumber, Δk, can be calculated by the equations from Eq. (5) to (11).

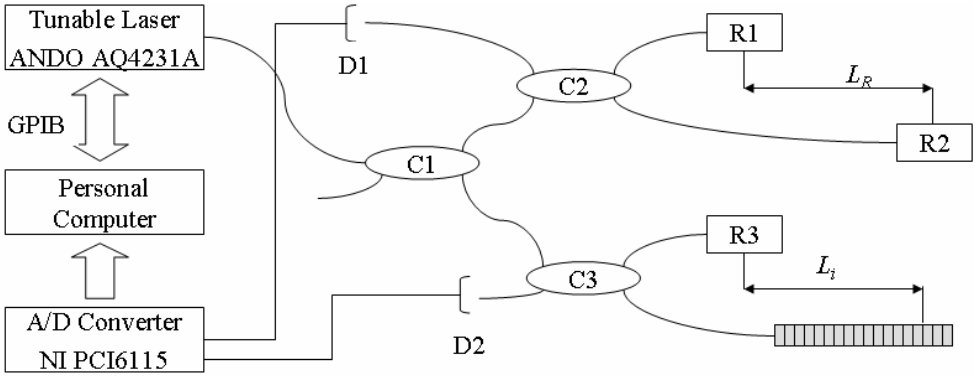

Figure 1: Schimatic of the measurement system

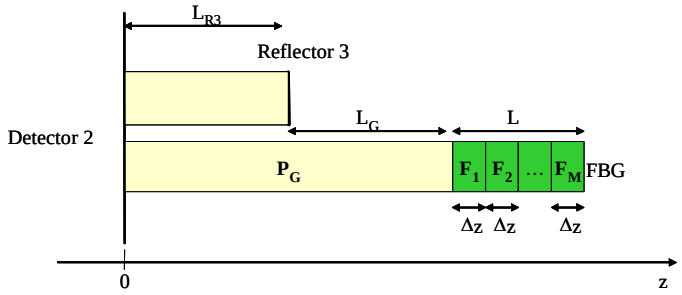

Figure 2: Interferometer model with FBG

Data analysis

As mentioned above, while the wavelength of the laser light from the tunable laser is swept, the signal at D2 in the interferometer consisted of a mirror end and a long gauge FBG is acquired at the constant wavenumber interval. This signal is represented by Eq. (6), and we can easily map the strain profile along the long gauge FBG from a spectrogaram given by applying Fourier transform analysis with a sliding window along the wavenumber axis to the D2 signal. We can predict that there is the wavenumber/length resolution trade-off inherent related to the uncertainty priciple. So a wide window gives better length (position) resolution but poor wavenumver (wavelength), while a narrower window gives good wavelength resolution but poor position resolution.

Simulation result

We simulated the D2 signal obtained from the measuremet system with the FBG whose gauge length was 100 mm and which was under the stress free condition, and we compared it with the experiment result. Figure 3 shows the D2 signals and the spectrograms obtained from the experiment and the simulation. In the simulation n, L_R, L_G and $\overline{\delta n}_{eff}$ the "dc" index change spatially averaged over a grating period are 1.45, 15.47 m, 4.96 m and 3.10×10^{-6}, respectively. The window length is 4000 points and it is corresponding to the wavenumber width of about 560 /m. The window was slid along the wavenumber axis as overlapping 3980 points.

The strain distribution can be found by determining the center wavelength of the spectrum at each position along the grating. As shown in the spectrograms of Fig. 3, we can see that the strain of the actual FBG is varying due to the manufacturing nonuniformity, while the strain distribution is uniform in the simulation result.

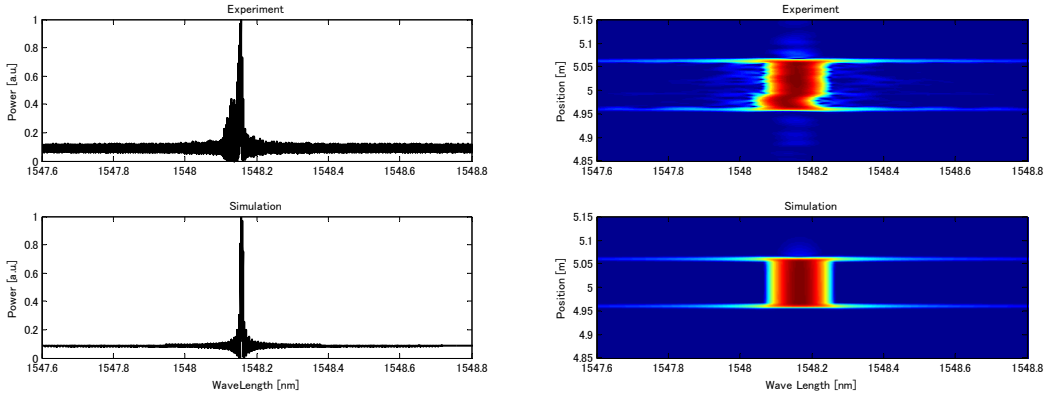

Fig. 3 D2 signals (left) and spectrograms (right) of the experiment and the simulation

DISTRIBUTED STRAIN SENSING IN STRESS CONCENTRATION ZONE

Stress concentration occurs frequently around a discontinuous site in the geometry or the material of a structure. It may cause fracture, and fracture may also cause it. Therefore, it is important technique to detect or measure stress concentration in structural health monitoring.

In this study, the strain distribution adjacent to holes of an aluminum tensile specimen was measured by the distributed strain sensing with OFDR. The aluminum specimen had a hole with the diameter of 4 mm and two holes with the diameter of 2 mm as shown in Fig. 4. An FBG sensor whose gauge length was 10 mm and whose coating was polyimide was bonded adjacent to the 4 mm hole to measure the strain distribution which was varying sharply by the stress concentration. Another FBG was also bonded on the other side along the holes. This FBG had 50 mm gauge length and the acrylate coating. In the experiments, the specimen was statically subjected to the tensile loads of 1.0, 2.0, 3.0, and 3.5 kN.

Figure 5 shows the strain distributions in the 3.0 kN load. The solid line is the strain distribution calculated by finite element method (FEM). By using our simulation model and the FEM result, we could estimate the strain distribution which would be measured by the sensing system. The estimated distribution is shown as the dashed line in Fig. 5. This result showed the potential to measure strain accurately. In fact, the agreement between the results of the FBG sensor with the polyimide coating and FEM is excellent. However, we cannot see the sharp variation in the strain distribution measured by the acrylate coating FBG. It is supposed that the interface between the cladding and the coating was affecting the spatial resolution in distributed strain sensing.

CONCLUSIONS

In this paper we showed that the distributed strain measurements with the high spatial resolution can be implemented by the new sensing technique based on OFDR. Strain profile along a long gauge FBG can be easily determined in a spectrogram calculated by applying Fourier transform analysis with a sliding window to the signal obtained from the measurement system. The strain distribution adjacent to holes of an aluminum tensile specimen was measured by the FBG with the polyimide coating and the FBG with the acrylate coating. The agreement between the experimental result of the polyimide coating FBG and the simulated one was good. This means that the simulation model was reasonable and can be used to design a measurement system with higher performance.

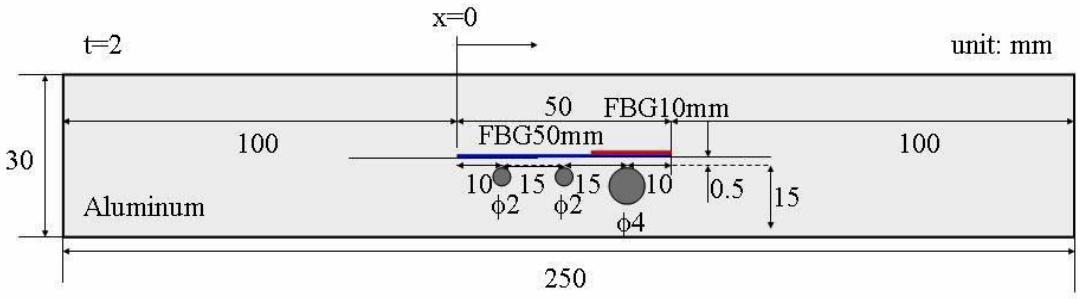

Figure 4: Tensile specimen with FBG sensors and holes

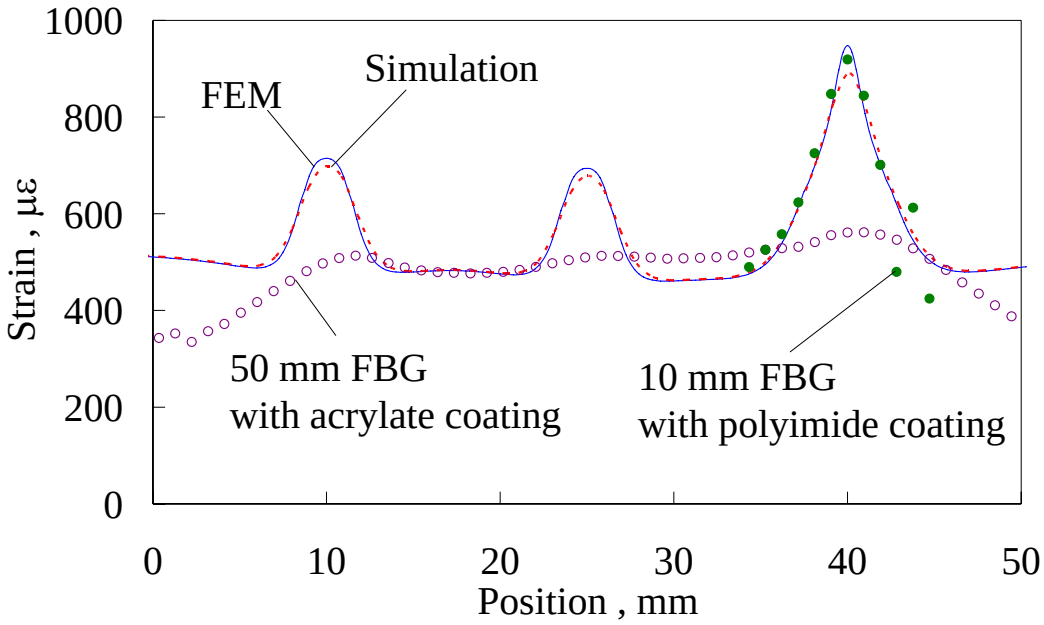

Figure 5: Strain distributions adjacent to the holes

REFERENCES

1. J. Dakin and B. Culshaw, Optical Fiber Sensors Volume Four: Applications, Analysis, and Future Trends, Artech House, pp.369-407 (1997)
2. M. LeBlanc, S. Y. Huang, M. Ohn and R. M. Measures, Distributed strain measurement based on a fiber Bragg grating and its reflection spectrum analysis, *Optics Letters*, Vol. 21, No. 17, pp.1405-1407 (1996)
3. M. Volanthen, H. Geiger and J. P. Dakin, Distributed grating sensors using low-coherence reflectometry, *Journal of Lightwave Technology*, Vol. 15, No. 11, pp.2076-2082 (1997)
4. S. Huang, M. M. Ohn and R. M. Measures, Phase-based Bragg intragrating distributed strain sensor, *Applied Optics*, Vol. 35, No. 7, pp.1135-1142 (1996)
5. R. M. Measure, M. M. Ohn, S. Y. Huang, J. Bigue and N. Y. Fan, Tunable laser demodulation of various fiber Bragg grating sensing modalities, *Smart Materials and Structures*, Vol. 7, No. 2, pp.237-247 (1998)
6. H. Igawa, H. Murayama, T. Kasai, I. Yamaguchi, K. Kageyama and K. Ohta, Measurements of strain distributions with a long gauge FBG sensor using optical frequency domain reflectometry, *Proc. of SPIE*, Vol. 5855, pp.547-550 (2005)
7. B. A. Childers, M. E. Froggatt, S. G. Allison, T. C. Moore, D. A. Hare, C. F. Batten and D. C. Jegley, Use of 3000 Bragg grating strain sensors distributed on four eight-meter optical fibers during static load tests of a composite structure, *Proc. of SPIE*, Vol. 4332, pp.133-142 (2001)
8. M. Froggatt, Distributed measurement of the complex modulation of a photoinduced Bragg grating in an optical fiber, *Applied Optics*, Vol. 35, No. 25, pp.5162-5164 (1996)
9. A. M. Abdi, S. Suzuki, A. Schülzgen and A. R. Kost, Fiber Bragg grating array calibration, *Proc. of SPIE*, Vol. 5765, pp.552-563 (2005)
10. T. Erdogan, Fiber Grating Spectra, *Journal of Lightwave Technology*, Vol. 15, No. 8, pp.1277-1294 (1997)